

Synthesis, DFT computational insights on structural, optical, photoelectrical characterizations and spectroscopic parameters of the novel (2E)-3-(4-methoxy-5-oxo-5H-furo[3,2-g]chromen-6-yl)acrylonitrile(MOFCA)



Shimaa Abdel Halim*, Magdy A. Ibrahim

Department of Chemistry, Faculty of Education, Ain Shams University, Roxy, 11711, Cairo, Egypt

ARTICLE INFO

Article history:

Received 5 August 2020

Revised 19 September 2020

Accepted 20 September 2020

Available online 23 September 2020

Keywords:

6-Formylvisnagin

DFT/TD-DFT

FT-IR spectrum

UV-Vis spectra

Optoelectronic application

ABSTRACT

Reaction of 6-formylvisnagin (**1**) with cyanoacetic acid in dry pyridine afforded the novel (2E)-3-(4-methoxy-5-oxo-5H-furo[3,2-g]chromen-6-yl)acrylonitrile (**2**, **MOFCA**). The chemical structure of the prepared compound was determined by the elemental analysis and spectral data. The individual emulsion characteristics of compound (**2**, **MOFCA**), were accomplished by DFT, and TD-DFT/B3LYP, at 6-311++G (d, p). The computational results detect the most stable structure of **MOFCA**, depending on the positions of the methoxy (O-CH₃) group, within change in dihedral angle. FT-IR spectroscopy was applied for the vibrational spectral analysis. Using frontier molecular orbital (FMO) analysis, various spectroscopic and quantum chemical parameters are discussed. The absorption energies, oscillator strength, and electronic transitions of compound (**2**, **MOFCA**), have been derived at TD-DFT/CAM-B3LYP/6-311++G (d,p) computations utilizing a PCM and measured in different polar and non-polar solvents experimentally in UV-Vis spectra. The output of the computation shows accurate agreement between theoretical spectra and practical spectra for the title compound. NLO analysis was computed at the identical plane of theory which are, α ; $\Delta\alpha$, and first-order β , the hyper-Rayleigh scattering (β_{HRS}) and the depolarization ratio (DR), were shown promising optical properties. The plots of natural bonding orbital (NBO), thermochemical parameters and the molecular electrostatic potential surfaces (MEPS) have been computed. All the computations in the gas phase have been completed.

© 2020 Elsevier B.V. All rights reserved.

1. Introduction

Fruits and seeds of Ammi visnaga L. represent the main source of the naturally occurring furochromones (khellin and visnagin) [1], and used for treating angina [2], psoriasis and vitiligo [3], kidney stones and as a spasmolytic agent [4]. They are broadly used as drugs for anti-inflammatory, analgesic [5,6], anticancer [7,8], anticonvulsants [9], antitubercular [10] and antimicrobial agent [11]. DFT-theoretical calculations have been studied geometrical optimized of some furo[3,2-g]chromenes[12,13]. Electronic spectra, molecular docking, computational, solvatochromic, photosensitivity, photoelectrical, photovoltaic, and photodiode studies were carried on a range of furo[3,2-g]chromenes [14–19]. Appropriately, it is suitable to synthesize the novel (2E)-3-(4-methoxy-5-oxo-5H-furo[3,2-g]chromen-6-yl) acrylonitrile (**2**, **MOFCA**), and study the

biological intrigue from the of view computational investigation [20]. The studied compound (**2**, **MOFCA**) is expected to have distinct biological properties that require exploration of its electronic structure in addition to its electronic and optical spectra. The present structure is classified as an organic semiconductor of small molecule, specified as a π -conjugated nanostructure structure, and has a delocalization of electrons as well as large extinction coefficient and good light gain. Accordingly, these types of materials have considerable attracting electrical and optical characteristics and appropriate for optoelectronic device applications [21].

Density functional theory-based computational study plays a vital role in identifying the new drug candidates and calculating the electronic structure of molecular systems. The accuracy and checking the experimental values of molecular geometry, vibrational frequencies, atomic charges, dipole moment, thermodynamically properties, etc. has been a favorite by DFT method [22–34].

According to our knowledge, there is no published work on the experimentally and computational vibrational spectroscopic (UV-Vis spectra) of the prepared compound (**2**, **MOFCA**). Therefore, the

* Corresponding author.

E-mail address: shimaaquantum@ymail.com (S.A. Halim).

present work interpret various results characteristics of **MOFCA** by offering the DFT/B3LYP/6-311++G(d, p) calculations of the molecular electrostatic potential, electronic absorption, and molecular vibrations analysis. The thermal analysis is also provided as well as the absorption coefficient analysis for the energy gap determination of **MOFCA**. Also, attempts to provide a comprehensive study of the UV-Vis spectra experimentally for the synthesized compound was calculated at CAM-B3LYP/6-311++G (d,p)by using Time-dependent density functional theory (TD-DFT).The natural bond orbital analysis (NBO) is described the charge transfer of the electron density in the studied compound. In addition, the present work displays the spectroscopic and thermodynamic properties, the electronic structure of the prepared compound (**2, MOFCA**).Based on theoretical chemistry; it has become possible to anticipate many physical and chemical properties of organic molecules. The thermo-chemical parameters, vibration harmonic frequencies, spectrum of FT-IR of compound (**2, MOFCA**) in the solid phase were recorded. Moreover, the electronic dipole moment (μ), first-order hyperpolarizability (β), hyper-Rayleigh scattering (β_{HRS}), and the depolarization ratio (DR), are parameters in non-linear optical (NLO), were calculated on the same level of theory. The spectrophotometric measurements explaining optical constants of the designed compound (**2, MOFCA**) are investigated, in a broad area of spectra.

2. Experimental

2.1. (2E)-3-(4-methoxy-5-oxo-5H-furo[3,2-g]chromen-6-yl)acrylonitrile(2, MOFCA)

A mixture of 4-methoxy-5-oxo-5H-furo[3,2-g]chromene-6-carboxaldehyde (**1**)(0.49 g, 2 mmol) and cyanoacetic acid (0.17 g, 2 mmol) in dry pyridine (10 mL) was stirred at room temperature for 1h. The reaction mixture was poured onto crushed ice (~ 20 g) and neutralized with conc. HCl. The yellow solid so obtained was filtered and crystallized from ethanol to give compound **2** as yellow crystals, yield (0.41 g, 77%), m.p. 239–240 °C. IR (KBr, cm^{-1}): IR (KBr, cm^{-1}):3112 ($\text{CH}_{\text{olefinic}}$), 3082 ($\text{CH}_{\text{arom.}}$), 2963, 2942 ($\text{CH}_{\text{aliph.}}$), 2218 ($\text{C}\equiv\text{N}$), 1643 ($\text{C}=\text{O}_\gamma\text{-pyrone}$), 1601 ($\text{C}=\text{C}$).¹H-NMR (400 MHz, DMSO- d_6 , δ): 3.98 (s, 3H, OCH_3), 6.81 (d, 1H, $J = 15.2$ Hz, $\text{H-}\alpha$ olefinic), 7.08 (d, 1H, $J = 2.4$ Hz, H-3furan), 7.19 (s, 3H, H-9), 7.33 (d, 1H, $J = 15.2$ Hz, $\text{H-}\beta$ olefinic), 7.91 (d, 1H, $J = 2.4$ Hz, H-2furan), 8.40 (s, 1H, H-7).¹³C-NMR (75 MHz, DMSO- d_6 , δ): 59.8 (OMe), 92.2 ($\text{C-}\alpha$ olefinic), 94.8 (C-9), 106.9 (C-3furan), 112.8 (C-4a), 114.1 (C-3a), 116.4 ($\text{C}\equiv\text{N}$), 118.0 (C-6), 146.6 (C-2furan), 148.8 (C-7), 151.0 (C- β olefinic), 154.5 (C-4), 159.2 (C-7a), 163.4 (C-9a), 176.8 (C-5 as C=O). Mass spectrum, m/z ($I_r\%$): 267 (M^+ , 65), 215 (48), 191 (24), 175 (17), 147 (44), 118 (100), 91 (59), 77 (42), 64 (18). Anal. Calcd for $\text{C}_{15}\text{H}_9\text{NO}_4$ (267.24): C, 67.42; H, 3.39; N, 5.24%. Found: C, 67.19; H, 3.33; N, 5.11%.

2.2. Apparatus

A digital Stuart SMP3 apparatus was used for melting points determination. FTIR Nicolet IS10 spectrophotometer (cm^{-1}) was applied for measuring the Infrared spectra, using KBr disks. Mercury-300BB apparatus was used for measuring the ¹H NMR (300 MHz) and ¹³C NMR (100 MHz) spectra, using DMSO- d_6 as a solvent and TMS (δ) as the internal standard. GC-2010 Shimadzu Gas chromatography instrument mass spectrometer (70 eV) was used for measuring the mass spectra. Elemental microanalyses were performed at Perkin-Elmer 2400II at the Chemical War Department, Ministry of Defense, and Egypt. The purity of the synthesized compounds was checked by thin layer chromatography and elemental microanalysis.

A Perkin Elmer lambda 4B spectrophotometer were used to measure the electronic absorption spectra using 1.0 cm fused quartz cells, and over the range of 200–900 nm. Spectral analysis of transmittance and reflectance is performed in the wavelength range of 200–750 nm.

2.3. Solvents

Merck, AR- grade were obtained the solvents, which Polar (methanol and butanol) and non-polar (dioxane and toluene), and were used without further purification.

2.4. Computational details

Intel (R) Core (TM) i7 computer were used for the Khon-Sham's (DFT) calculations by the Gaussian-09 program package without any constraint on the geometry [35]. The geometry of the molecules studied in this is optimized by DFT/B3LYP method using a 6-311++G (d, p) basis set [36–38]. The FMO analysis and quantum chemical study has been performed using Gauss View 5.0.9 [39] or chem. craft 1.6 [40] software packages. Also, the following equations [41–43] were calculated the total static dipole moment (μ), $\langle \Delta\alpha \rangle$, and $\langle \beta \rangle$, values.

$$\begin{aligned} \mu &= (\mu_x^2 + \mu_y^2 + \mu_z^2)^{1/2}, \\ \langle \alpha \rangle &= 1/3(\alpha_{xx} + \alpha_{yy} + \alpha_{zz}), \\ \Delta\alpha &= ((\alpha_{xx} - \alpha_{yy})^2 + (\alpha_{yy} - \alpha_{zz})^2 + (\alpha_{zz} - \alpha_{xx})^2/2)^{1/2}, \\ \langle \beta \rangle &= (\beta_x^2 + \beta_y^2 + \beta_z^2)^{1/2}, \end{aligned} \quad (1)$$

$$\begin{aligned} \text{Where } \beta_x &+ \beta_{xxx} + \beta_{xyy} + \beta_{xzz}, \\ \beta_y &+ \beta_{yyy} + \beta_{xxy} + \beta_{yzz}, \\ \beta_z &+ \beta_{zzz} + \beta_{xzz} + \beta_{yyz}, \end{aligned} \quad (2)$$

The hyper-Rayleigh scattering (β_{HRS}) and depolarization ratio (DR) [44] are parameters for the second-order NLO; which calculated as:

$$\beta(\text{HR}_s) = \sqrt{\beta^2 zzz + \beta^2 zxx} \quad (3)$$

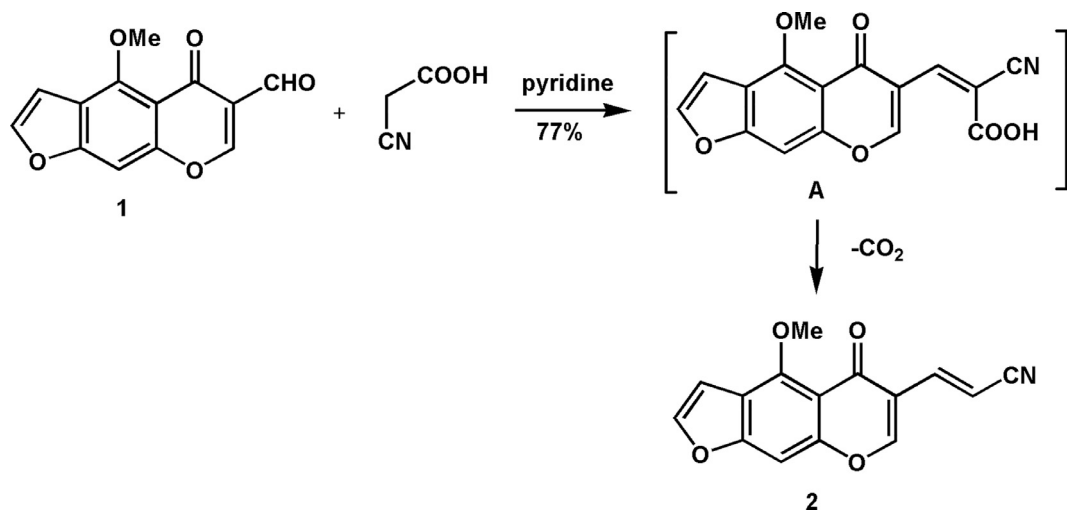
$$\text{DR} = \frac{\beta^2 zzz}{\beta^2 zxx} \quad (4)$$

The deviation in the amounts of β_{HRS} and DR can be recognized by structural index [45]. Using the predicted energies of HOMO and LUMO, global reactivity descriptors were calculated as follows: $\chi = (I + A)/2$ (electronegativity), $\eta = (I - A)/2$ (chemical hardness), $S = 1/2\eta$ (global softness), $\omega = \mu^2/2\eta$ (electrophilicity) where I and A were ionization potential and electron affinity, and $I = -E_{\text{HOMO}}$ and $A = -E_{\text{LUMO}}$, respectively [46,47]. Absorption energies (λ in nm), Oscillator strength (f), and Transitions of the compound (**2, MOFCA**) has been calculated at TD-CAM-B3LYP/6-311++G (d, p) level of theory [48,49].

3. Results and discussion

3.1. Chemistry

The novel (2E)-3-(4-methoxy-5-oxo-5H-furo[3,2-g]chromen-6-yl)acrylonitrile(**2**) was prepared by reacting 6-formylvisnagin (**1**) with cyano acetic acid in dry pyridine (**Scheme 1**) [20]. Formation of compound (**2, MOFCA**) may proceed through condensation of the aldehyde functional group with the active methylene group giving intermediate **A**, which underwent decarboxylation under the reaction conditions. The IR spectrum of compound (**2, MOFCA**) (**Fig. 1**) showed distinctive absorption bands at 2218 ($\text{C}\equiv\text{N}$) and 1643 cm^{-1} ($\text{C}=\text{O}_\gamma\text{-pyrone}$). The ¹H-NMR spectrum of compound (**2, MOFCA**) (**Fig. 2**) revealed two characteristic doublets ($J = 15.2$ Hz)



Scheme 1. Formation of the novel acrylonitrile derivative (2, MOFCA).

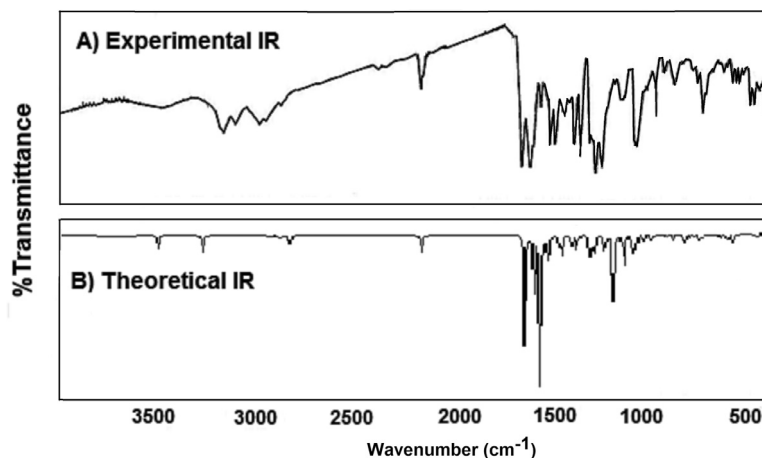
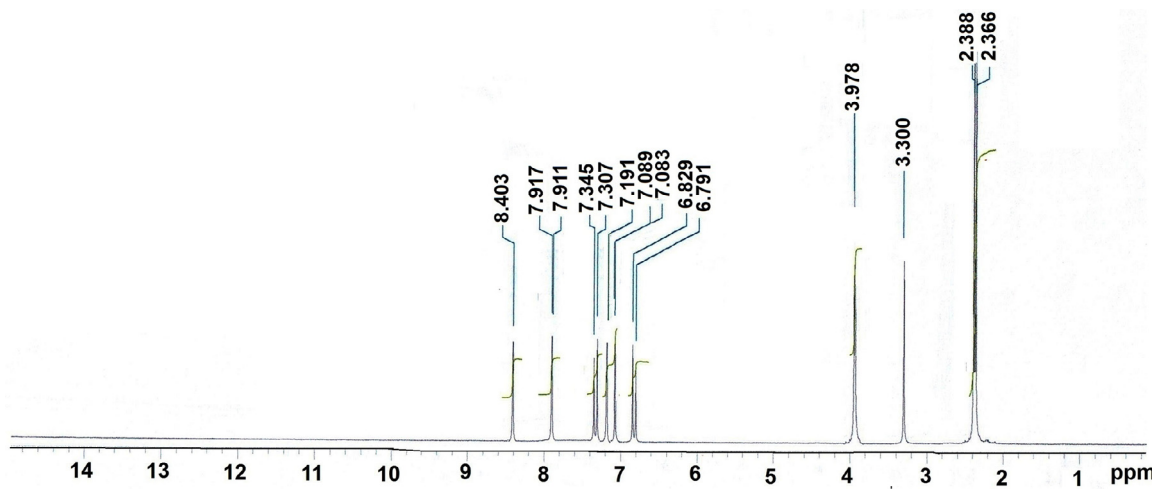


Fig. 1. Experimental and Calculated IR spectra of compound (2, MOFCA) at B3LYP/6-311++G (d,p).

Fig. 2. The ^1H NMR spectrum of compound (2, MOFCA).

assignable to the vinyl protons at δ 6.81 and 7.33 ppm, the high coupling constant indicates *trans* configuration around the double bond. Also, the doublet signals ($J = 2.4$ Hz) attribute able to H-3_{furan} and H-2_{furan} were observed at δ 7.08 and 7.91 ppm, respectively. Characteristic singlet signals appeared at δ 7.19 and 8.40 which assignable to H-9 and H-7, respectively. The ^{13}C NMR spec-

trum of compound (2, MOFCA) (Fig. 3) agrees well with the proposed structure and recorded fifteen signals corresponding to the number of carbon atoms present in the synthesized compound 2. These signals were explained as follows; 59.8 (O-Me), 92.2 (C- α _olefinic), 94.8 (C-9), 106.9 (C-3_{furan}), 112.8 (C-4a), 114.1 (C-3a), 116.4 (C≡N), 118.0 (C-6), 146.6 (C-2_{furan}), 148.8 (C-7), 151.0 (C-

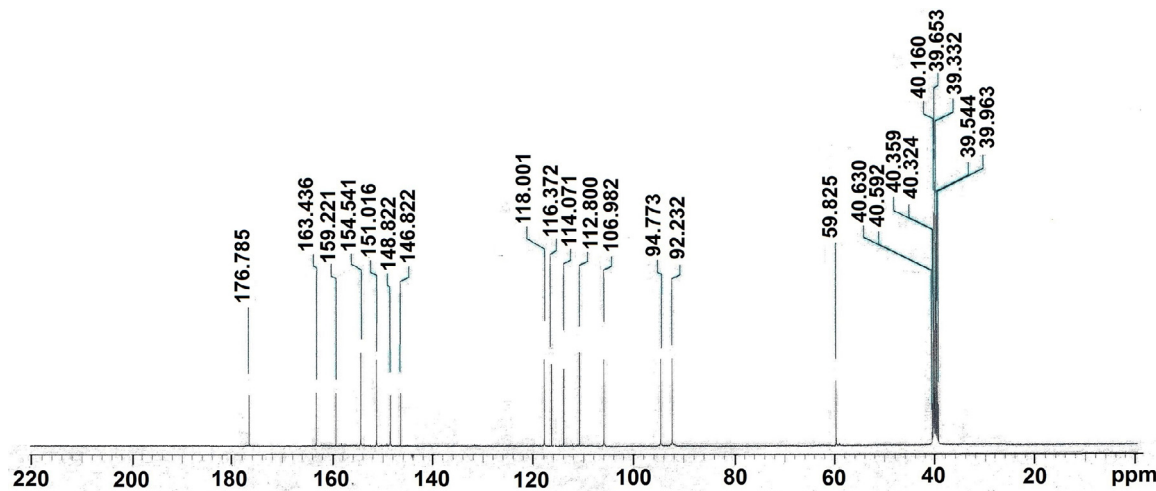
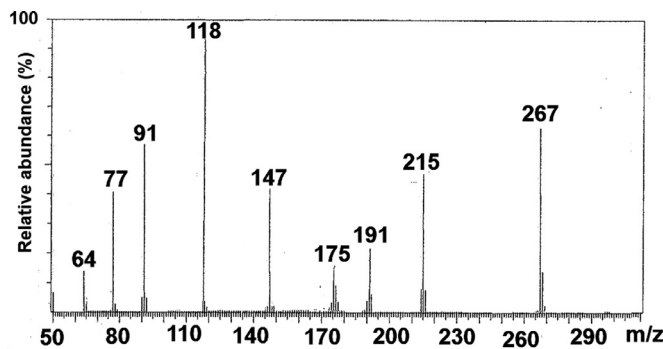
Fig. 3. The ^{13}C NMR spectrum of compound (2, MOFCA).

Fig. 4. The mass spectrum of compound (2, MOFCA).

β -olefinic), 154.5 (C-4), 159.2 (C-7a), 163.4 (C-9a), 176.8 (C-5 as C=O). The mass spectrum of compound (2, MOFCA) (Fig. 4) revealed its molecular ion peak at m/z 267 and supports the identity of the structure. The mass fragmentation patterns of compound 2 are depicted in Scheme 2.

3.2. Electronic structures

3.2.1. Computational stability of MOFCA

At the optimized geometry for the stability of compound **MOFCA**, four different conformers (**1-4**) are expected, depending on the positions of the methoxy (O-CH₃) group, whether it is directed away from or toward the ring, which was chosen to investigate the possible conformers of the **MOFCA** molecule, within the change in dihedral angle using the Gaussian program. The computational results detect the most stable conformer of the **MOFCA**, as the conformer (**4**) has minimum energy, as shown in Fig. 5. Both forms of the molecule are in the same plane. However, Tables and Figures were prepared only for the most stable conformer (**4**). The theoretical geometric structures with atoms the numbering of compound (2, MOFCA) are shown in (Fig. 5). The difference in energy of 0.0002 a.u.; (0.00544 eV); (0.1254 kcal); for conformer (**3**), which less stable than conformer (**4**), by change in D.A = 122.51° and so on; it's also more stable by 0.0123 a.u.; (0.335 eV); (7.7116 kcal); than conformer (**2**), as well than conformer (**1**), by 0.0671 a.u.; (1.825 eV); (42.0690 kcal).

3.2.2. Geometry, ground states and global properties of MOFCA

The novel compound (2, MOFCA) has been studied to determine various structural and chemical parameters using density func-

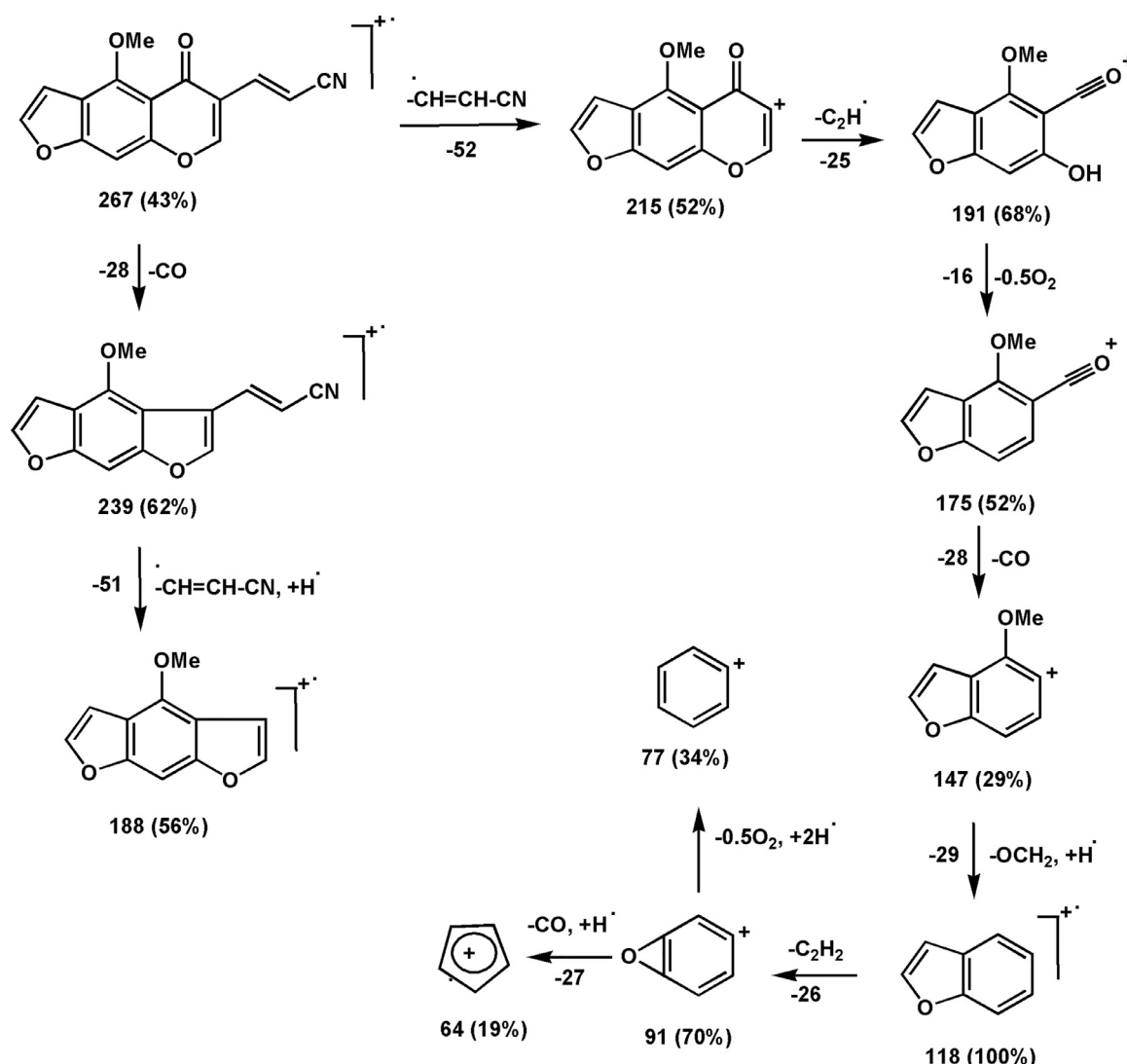
Table 1

The optimized calculations of (2E)-3-(4-methoxy-5-oxo-5H-furo[3,2-g]chromen-6-yl) acrylonitrile (MOFCA) at the B3LYP/6-311++G (d,p).

Parameters	MOFCA
Total Energy (E _T), (a. u.)	-932.8363
Zero Point Vibrational Energy(kcal/mol)	127.330
	0.85808
Rotational constant(GHz)	0.15005
0.17846	
Total Entropy (cal/mol. K)	129.912
Translational	41.810
Rotational	33.238
Vibrational	54.864
Energy of highest occupied molecular orbital (E _{HOMO}) (eV)	-6.556
Energy of lowest unoccupied molecular orbital (E _{LUMO}) (eV)	-2.536
Energy gap(E _g) (eV)	4.020
E _{HOMO} -1(eV)	-7.273
E _{LUMO} +1(eV)	-2.148
Energy gap(E _g) (eV)	5.124
E _{HOMO} -2(eV)	-7.460
E _{LUMO} +2(eV)	-1.285
Energy gap(E _g) (eV)	6.175
Dipole moment, (μ)	7.8870
I (eV)	6.55602
A(eV)	2.53586
X(eV)	4.54594
V(eV ⁻¹)	-4.54594
η (eV)	2.01008
S(eV ⁻¹)	0.24875
ω (eV)	5.14048

tional theory DFT/B3LYB at 6-311++G (d,p) basis set (Fig. 6), and having C1 point group symmetry as predicted by DFT investigation. The frontier molecular orbital's (FMO) of synthesized compound (2, MOFCA) is presented in Fig. 7, the electronic parameters and the global reactivity descriptors statistics are given in Table 1. The investigation of Table 1, and Figs. 6 and 7 clarifies the following:

The C-C bond lengths in a typical aromatic six-member ring (Ca. 1.39 Å) is indicator for comparison with C-C and C=C, computed bond lengths which larger and shorter significantly. Alright, the central bond in butadiene (1.463 Å) [50], which found to be similar to the C-C bond lengths for compound (2, MOFCA) (1.449–1.479 Å), while the C=C bond lengths (1.387–1.390 Å) did not differ highly from the C=C bond length in ethylene [51]. The considerably large O-C bond lengths and shorten C=O bond length were suggested in these conclusions. The small difference between calculated and observed bond lengths indicated the power of the method used in the calculation. No considerable change in the cal-



Scheme 2. The mass fragmentation patterns of compound (2, MOFCA).

culated bond angles of the compound on comparing with the experimental values (Fig. 6). The small difference between calculated and observed angles may be attributed to that the calculations were carried out in the gas phase and observed in the solid state. Also, compound (**2, MOFCA**) is planner, as reflected from their dihedral angles except for the methoxy group and ethylene group, which are out from the planarity (Fig. 6). The ionization energy, the electron affinity, the HOMO-LUMO gap, and the dipole moment, are the most important parameters which were evaluated in Table 1 and Fig. 7.

The Frontier molecular orbital analysis (FMOs) collected by HOMO and LUMO forms, and they are a role during molecular interactions between atomic orbitals. FMOs have indicator for the optical properties, electronic properties and reactivity of the molecule under investigation. In our case, FMO analyses were accomplished to omen the electronic properties of **MOFCA** at DFT/B3LYP/6-311++G(d,p),from the results of FMOs analysis they are hold four molecular orbital pairs, their gap energies, and are given in Table 1. The lower energy gap is 4.020 eV in **MOFCA**, when the electron transfer from HOMO-orbital → LUMO-orbital while the highest energy gap value 6.175 eV is spotted in **MOFCA** at HOMO-2→ LUMO+2. From Fig. 7, it is clear those HOMOs in **MOFCA** are over the molecule. Other with, LUMOs are centered through all atoms and slightly on the acrylonitrile group.

The global descriptor study suggests the compound (**2, MOFCA**) is good electrophiles as the value of global electrophilicity, (ω) is less. The synthesized molecule has greater kinetic stability and electron-donating capability, (χ), with chemically hard (η).

3.3. Non-linear Optical Properties (NLO)

The total static dipole moment (μ), mean polarizability ($\langle\alpha\rangle$), anisotropy of the polarizability ($\Delta\alpha$), mean first-order hyperpolarizability ($\langle\beta\rangle$), depolarization ratio (DR), and Hyper-Rayleigh scattering (β_{HRS}) were listed in Table 2 by using B3LYP / 6-311 ++ G (d, p). The NLO for compound (**2, MOFCA**) has no practical values, so urea was chosen as a reference [52]. The size of the molecular polarization ($\langle\beta\rangle$) is one of the main factors in the NLO system; also the lowest value of β , DR, and the highest value of β_{HRS} for the studied compound confirm short bond length which confirms their higher selectivity. Consequently, the process of converting solar energy is an important intermediary for NLO application for compound (**2, MOFCA**) [53]. A comparison of the obtained results for all factors with those published for the similar structures are listed in Table 3. The values of the obtained parameters for **MOFCA** are close to the values obtained for the similar structures, taking into account the computational error percent, which confirms the accuracy of the obtained results [54–56].

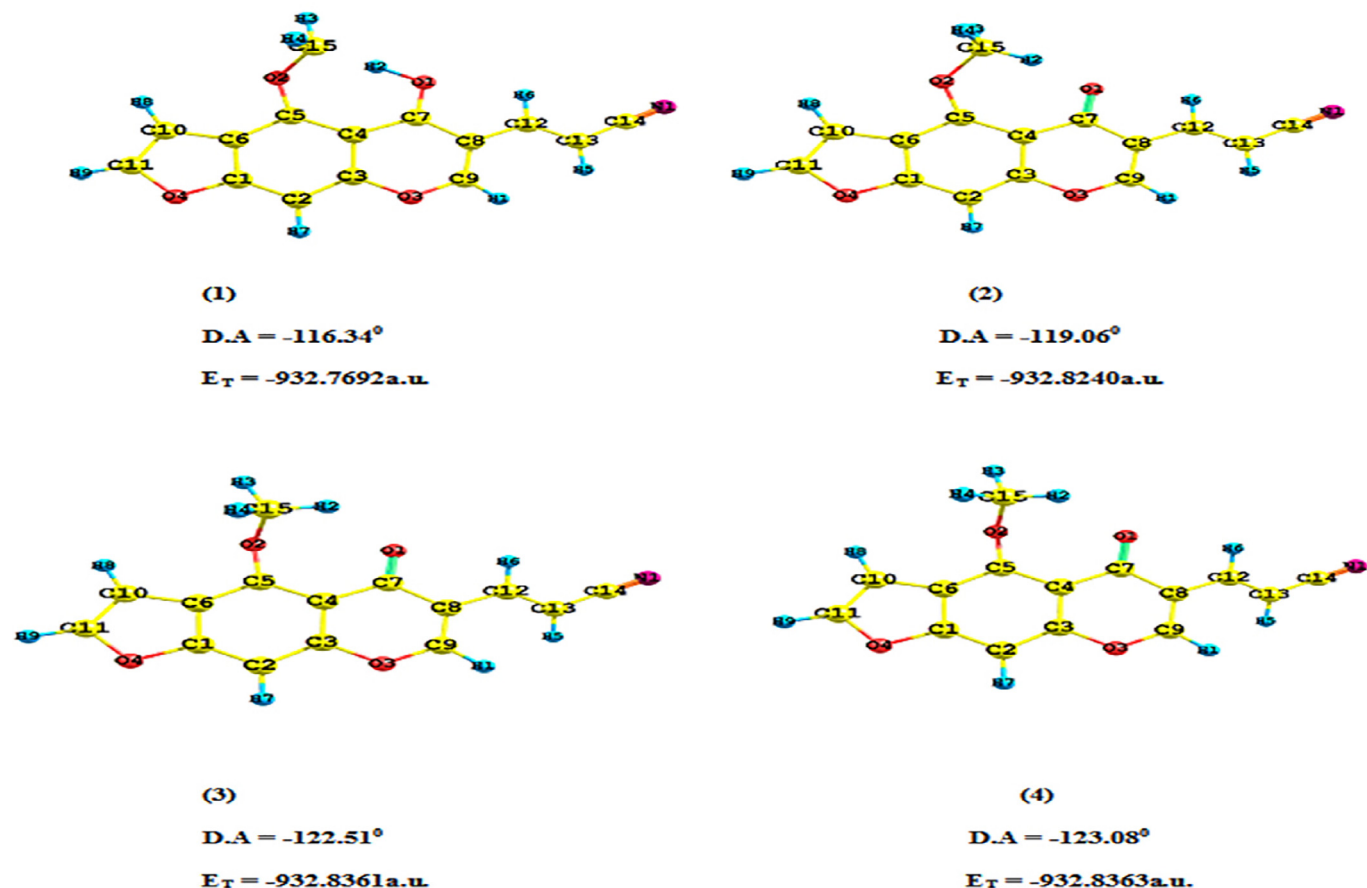


Fig. 5. Different dihedral angle using Gaussian program within the MOFCA structure

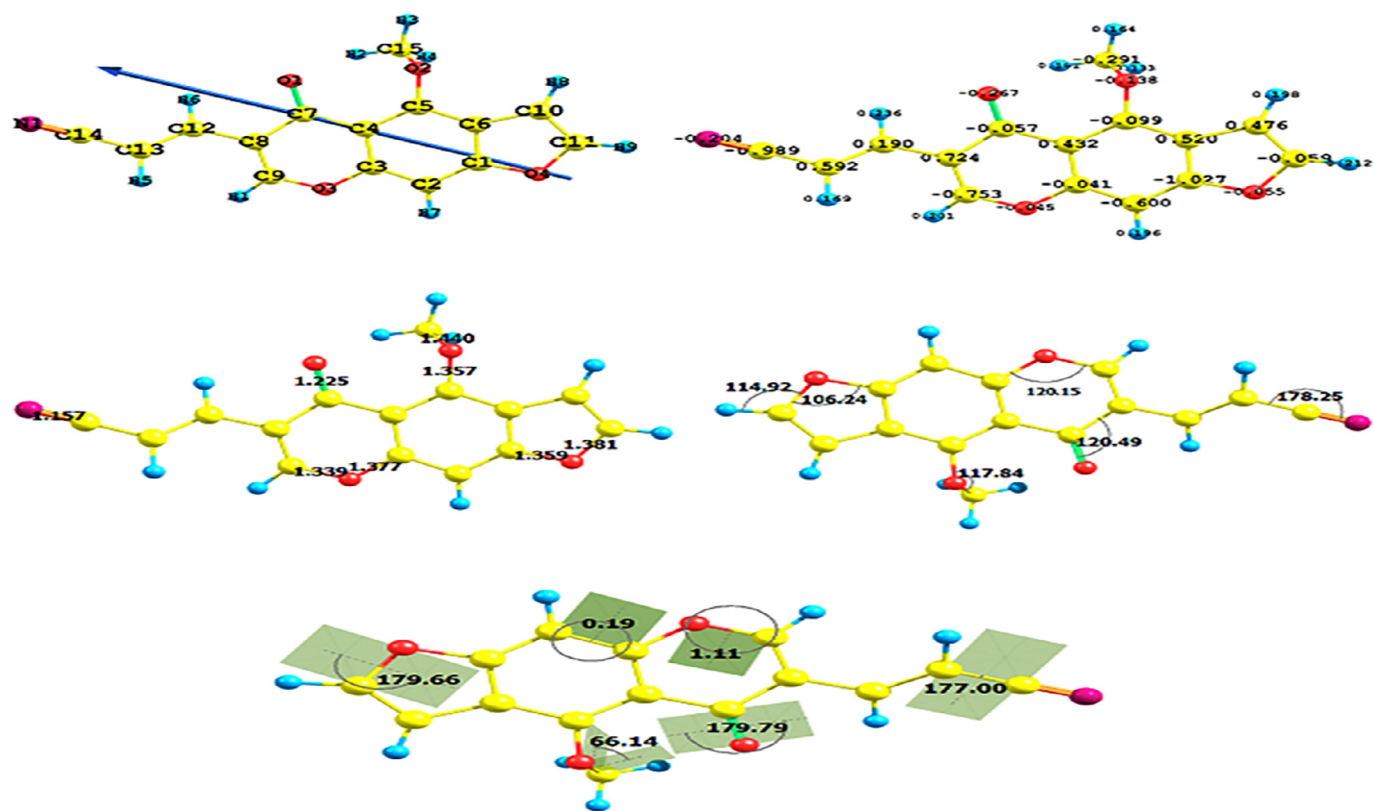


Fig. 6. The optimized structure, numbering system, perspective view of dipole moment, natural charge, the bond length, the bond angle and the dihedral angle of compound 2, MOFCA at B3LYP/6-311++G (d, p).

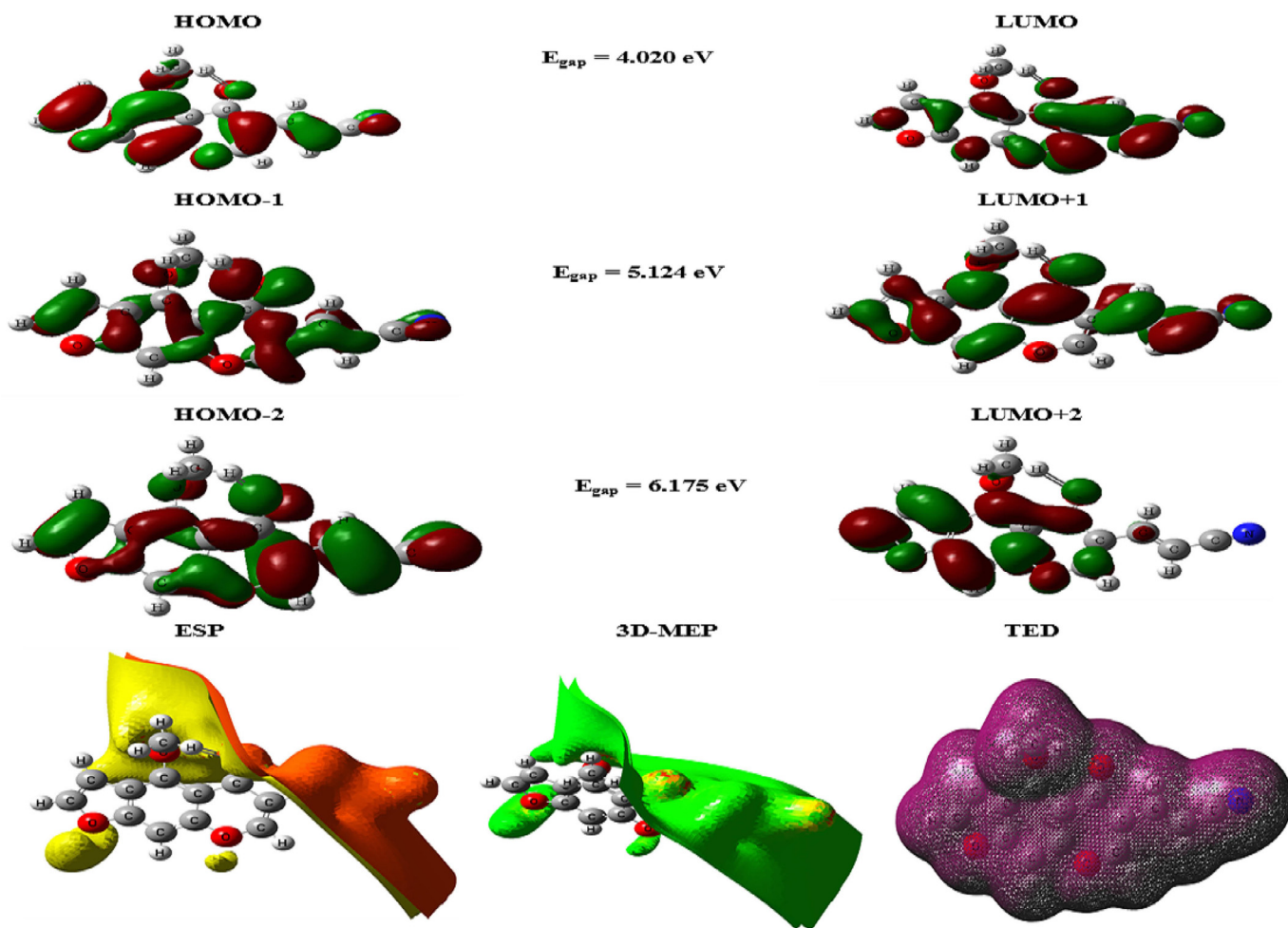


Fig. 7. HOMO, LUMO and Molecular surfaces ESP, 3D-MEP and TED of compound (2, MOFCA) at B3LYP/6-311++G (d,p).

3.4. Molecular electrostatic potential calculation

The molecular electrostatic potential (MEP) is associated with electrophilic and nucleophilic of the electronic density and careful the sites for the hydrogen-bonding interactions [57]. The charge distributions defining how molecules interact with each other and useful for visualizing the variable. Also, the electronic density has been related to the dipole moments, electrical negativity, and the chemical reactivity of molecules. Fig. 7 and Fig. S1 offers the optimized molecular structure studied for 3D-MEP and ESP of the **MOFCA** by using DFT/B3LYP/6-311++G (d,p).

The atomic sites O and N display the distribution of the lone pair of electron in the negative region were represented in red, furthermore the positive sites is around the hydrogen and carbon atoms (blue) [58,59].

3.5. Natural bond orbital (NBO) analysis

The natural bond orbital method (NBO) [60] used to investigate the reactive sites of the prepared compound (**2, MOFCA**), the molecular electrostatic potential (MEP) was computed. The donor-acceptor interactions were used to evaluate the second-order Fock matrix [61]. For each donor (i) and acceptor (j), the stabilization energy $E^{(2)}$ associated with the delocalization $i \rightarrow j$ was estimated as:

$$E^{(2)} = \Delta E_{ij} = q_i (F(ij)^2 / \varepsilon_j - \varepsilon_i), \quad (5)$$

Where q_i is the donor orbital occupancy, ε_i , and ε_j are diagonal elements and (ij) is the off-diagonal NBO Fock matrix element. The delocalization trend of electrons is related to the higher $E^{(2)}$ value, and thus stronger interaction at donor to acceptor orbital's. The selected NBO of the optimized structures are listed in Table 4. Higher values of the stabilization energies for $\pi\text{C}_3\text{-C}_4 \rightarrow \text{RY}^*\text{N}_20$, $\pi\text{C}_1\text{C}_2\text{-H}_29 \rightarrow \text{RY}^*\text{H}_28$, $\pi\text{C}_1\text{N}_20 \rightarrow \text{RY}^*\text{H}_28$, $\pi\text{C}_3\text{-C}_4 \rightarrow \text{RY}^*\text{C}_12$, $\pi\text{C}_3\text{-C}_4 \rightarrow \pi^*\text{C}_13\text{-C}_14$, $\pi\text{C}_1\text{-O}_19 \rightarrow \text{RY}^*\text{N}_20$, and $\pi\text{C}_1\text{-O}_19 \rightarrow \pi^*\text{C}_12\text{-H}_29$, interactions are achieved in geometry of compound (**2, MOFCA**). The large stabilization effects are due to the strong lone pair-anti-bonding orbital interactions between the two ends of the formed H-bond. These results indicate that; the compound (**2, MOFCA**) structure has a stronger H-bond with the methoxy group. Hence, the structure becomes stronger stabilization of **MOFCA**.

3.6. Natural charges and natural population analysis

The natural electronic configuration of active sites for **MOFCA** at the B3LYP/6-311++G (d,p), presented in Table 5, which also, contains the natural charge, natural population, natural population of the total electrons on the sub-shells. The more positive atoms of electricity tended to accept an electron. Whilst the most negative center atoms were the O16, O17, O18, O19, and N20 atoms, head to suggest a private electron from the static electricity of the **MOFCA** molecule. Furthermore, there are 138 electrons in **MOFCA** are co-

Table 2

Total static dipole moment (μ), mean polarizability ($\langle\alpha\rangle$), anisotropy of the polarizability ($\Delta\alpha$), and mean first-order hyperpolarizability ($\langle\beta\rangle$), for MOFCA at the B3LYP/6-311++G (d,p).

Property	(MOFCA)
μ_x , D	-7.1930
μ_y , D	-2.8571
μ_z , D	1.5171
μ , Debye ^a	7.8870
α_{xx} , a.u.	-145.3630
α_{xy} , a.u.	-15.8144
α_{yy} , a.u.	-108.3690
α_{xz} , a.u.	-115.8166
α_{yz} , a.u.	4.1551
α_{xz} , a.u.	2.5534
$\langle\alpha\rangle \times 10^{-24}$ esu	36.813
$\Delta\alpha \times 10^{-24}$ esu	44.650
β_{xxx} , a.u.	-509.0839
β_{xxy} , a.u.	-42.8278
β_{xyy} , a.u.	-7.6781
β_{yyy} , a.u.	5.7606
β_{xxx} , a.u.	6.1788
β_{xyz} , a.u.	1.2666
β_{yyz} , a.u.	12.1241
β_{zzz} , a.u.	-4.0787
β_{yzz} , a.u.	2.6035
β_{zzz} , a.u.	1.9100
$\langle\beta\rangle \times 10^{-30}$ esu ^b	3.5861
DR	0.44
β_{HRS}	55.21

^a

^b Urea equal (1.3197D, 0.1947esu) results are taken from references [52].

Table 4

The significant E⁽²⁾ values (kcal/mol) for the optimized structure MOFCA of the selected interactions in the NBO analysis at the B3LYP/6-311++G (d,p).

Charge transfer	E ^{(2)a} (kcal/mol)	NBO	Population
$\pi C3-C4 \rightarrow RY^*C12$	5790.05	$\pi C2-C3$	1.96936
$\pi C2-C3 \rightarrow RY^*H29$	249.92	$\pi C3-C4$	1.97181
$\pi C3-C4 \rightarrow \pi^*C13-C14$	5497.46	$\pi C13-C14$	1.81156
$\pi C1-O19 \rightarrow RY^*C1$	14.93	$\pi C12-H29$	1.97923
$\pi C1-O19 \rightarrow RY^*O19$	31.75	RY^*C12	0.00577
$\pi C1-O19 \rightarrow RY^*N20$	3749.69	RY^*H29	0.00029
$\pi C1-O19 \rightarrow RY^*H28$	350.77	RY^*O19	0.00363
$\pi C1-O19 \rightarrow \pi^*C13-C14$	205.55	RY^*N20	1.99074
$\sigma C1-O19 \rightarrow \pi^*C9-O18$	105.49	$\pi C1-O19$	1.95524
$\pi C1-O19 \rightarrow \pi^*C12-H29$	3670.76	$\pi C15-N20$	1.99878
$\pi C1-O19 \rightarrow \sigma^*C15-N20$	28.78	CR C1	1.99976
$\sigma C3-C4 \rightarrow RY^*O19$	50.10	CR O17	1.99976
$\pi C3-C4 \rightarrow RY^*N20$	9077.49	LP O19	1.97256
$\pi C3-C4 \rightarrow RY^*H29$	253.76		
$\pi C3-C4 \rightarrow \pi^*C9-O18$	130.95		
$\pi C3-C4 \rightarrow \pi^*C12-H29$	1953.12		
$\pi C3-C4 \rightarrow \pi^*C15-N20$	1630.37		
$\pi C12-H29 \rightarrow RY^*C2$	1655		
$\pi C12-H29 \rightarrow RY^*H28$	9629.08		
$\pi C15-N20 \rightarrow RY^*C1$	3595.48		
$\pi C15-N20 \rightarrow RY^*H28$	7206.74		
$\pi C15-N20 \rightarrow \pi^*C15-N20$	280.18		
CR C1 $\rightarrow RY^*C12$	187.51		
CR C1 $\rightarrow RY^*H29$	68.64		
CR C1 $\rightarrow \pi^*C13-C14$	476.29		
CR C1 $\rightarrow \pi^*C15-N20$	1758.02		
CR O17 $\rightarrow RY^*C9$	89.95		
CR O17 $\rightarrow RY^*H29$	126.98		
CR O17 $\rightarrow \pi^*C15-N20$	368.10		
LP O19 $\rightarrow RY^*H28$	158.08		
LP O19 $\rightarrow RY^*C9$	165.21		

^aE⁽²⁾ means energy of hyperconjugative interactions (stabilization energy). LP_(n) is a valence lone pair orbital (n) on atom.

ordinated in sub-shells as a total Lewis and a total non-Lewis in natural population analysis.

3.7. Vibrational calculation characteristics

The calculated and experimental vibrations found repulsion between them, because of the calculations are done in a gas state. A comparison of the calculated vibration frequencies at DFT/B3LYP/6-311 ++ G (d, p) with those for the experimental values and related assignments from FT-IR spectra from MOFCA are illustrated in Fig. 1, and Table 6. As a result, the un-scaled calculated frequency was obtained. To improve the calculated values in agreement with the experimental values, a spectral uniform scaling factor was used to offset the systematic errors caused by basis set incompleteness, neglect of electron correlation, and vibrational harmonicas. Hence, the vibrational frequencies calculated at B3LYP/6- 311++G (d,p) level are scaled by 0.9613. After scaled with the scaling factor, the deviation from the experiments is less than 10 cm⁻¹ with

a few exceptions. The assignment can be implemented on a wide scale as follows:

The region 3000–3100 cm⁻¹ appeared the aromatic expansion vibrations (C–H) [62], and the computed vibration of the C–H aromatic is at 3170 cm⁻¹ (un-scaled value) and 3047 cm⁻¹ (scaled value) and experimentally observed at 3082 cm⁻¹. While, experimentally for the C–H symmetric aliphatic stretching vibration in CH₃ at 2963, 2942 cm⁻¹, and calculated at 2997, 2920 cm⁻¹ (unscaled value), and 2881, 2807 cm⁻¹, (scaled value) respectively, for compound (2, MOFCA).

The experimental C–H twisting vibration was observed at 3112 cm⁻¹, which agreed with the computed vibration at 3240 cm⁻¹ (un-scaled value) and at 3115 cm⁻¹ (scaled value). Generally, the observed C=O vibrations were in the range of 1790–1810 cm⁻¹[63], and found experimentally at 1643cm⁻¹, while theoretically at

Table 3

A comparative analysis of MOFCA with similar type of compounds.

Parameters	(MOFCA)	Ref.[54]	Ref.[55]	Ref.[56]
Energy of highest occupied molecular orbital (EHOMO)	-6.556	-4.89	-6.4355	-6.087
Energy of lowest unoccupied molecular orbital (ELUMO)	-2.536	-1.496	-2.3147	-1.824
Energy Gap(Eg)	4.020	3.393	4.1208	4.263
Dipole moment, (μ)	7.8870	6.5231	7.2563	7.8521
I (eV)	6.55602	4.89	6.4355	6.087
A(eV)	2.53586	1.496	2.3147	1.824
X(eV)	4.54594	3.193	4.3751	3.955
V(eV-1)	-4.54594	-3.193	-4.3751	-3.955
η (eV)	2.01008	1.6965	2.0604	2.1315
S(eV-1)	0.24875	0.29472	0.24267	0.23458
ω (eV)	5.14048	3.004789	4.645093	3.669253

Table 5
Natural charge, natural population analysis for MOFCA at the B3LYP/6-311++G (d,p).

Atom No.	Natural Charge	Natural Population Core	Valence	Rydberg	Total	Natural electronic Configuration
O16	-0.58513	1.999	6.5722	0.01311	8.585	[core]2S(1.69)2p(4.88)3p(0.01)
O17	-0.55921	1.999	6.5370	0.02246	8.559	[core]2S(1.59)2p(4.95)3p(0.01)
O18	-0.46882	1.999	6.4511	0.01805	8.469	[core]2S(1.57)2p(4.88)3p(0.01)
O19	-0.46847	1.999	6.4534	0.01535	8.468	[core]2S(1.60)2p(4.86)3p(0.01)
N20	-0.31608	1.999	5.2957	0.02075	7.316	[core]2S(1.59)2p(3.71)3d(0.01)
Core						39.98257 (99.956% of 40)
Valence Lewis						94.84059 (96.776% of 98)
Total Lewis						134.82316 (97.698% of 138)
Valence non-Lewis						2.88897 (2.093% of 138)
Rydberg non-Lewis						0.28787 (0.209% of 138)
Total non-Lewis						3.17684 (2.302% of 138)

Table 6
Experimental and computational calculated vibrational wavenumbers (harmonic frequency (cm^{-1})), (scaled and un-scaled values), IR intensities and assignments for MOFCA at the B3LYP/6-311++G (d,p).

No.	Exp.	Wave number un-scaled	Wave number scaled	IR Intensity Rel.	IR Intensity Abs.	Assignments	References
1	3112	3240	3115	55.58	21.57	ν C-H olefin	[62]
2	3082	3170	3047	21.84	12.84	ν C-H _{aromatic}	[62]
3	2963, 2942	2997, 2920	2881, 2807	26.22	16.72	ν C-H aliphatic	[62]
4	1643	1740	1673	119.62	87.35	ν C=O γ -pyrone	[63]
5	2218	2250	2189	21.47	45.26	ν C≡N	[63]
6	1601	1650	1605	107.25	52.16	β C=C (in ring)	[63]

ν Twisting (Stretching); ν_2 (Symmetric stretching); ν_3 (Asymmetric stretching); β (In plane bending).

Table 7
Thermodynamic properties at different temperatures for MOFCA at the B3LYP/6-311++G (d,p).

$S^\circ_m(\text{calmol}^{-1}\text{K}^{-1})$	$C^\circ_{\text{p,m}}(\text{calmol}^{-1}\text{K}^{-1})$	$H^\circ_m(\text{kcalmol}^{-1})$	T (K)
120.10	50.80	116.14	200
132.96	60.74	118.93	250
145.23	69.93	122.20	300
156.95	78.31	125.91	350
168.18	85.87	130.01	400
178.92	92.64	134.48	450
189.21	98.66	139.27	500
199.06	104.00	144.33	550
208.49	108.75	149.66	600

1740 cm^{-1} , (un-scaled value) and at 1673 cm^{-1} , (scaled value) for compound (2, MOFCA).

The vibration of C=C is generally detected in the range 1480–1630 cm^{-1} [63], and experimentally, recorded at 1601 cm^{-1} , these agreement with computed vibration at 1650 cm^{-1} , (un-scaled value) and at 1605 cm^{-1} , (scaled value). Also; the calculated asymmetric vibration of C≡N is showed at 2250 cm^{-1} , (un-scaled value) and at 2189 cm^{-1} (scaled value), which agreement with experimental results at 2218 cm^{-1} .

3.8. Electronic UV-spectra

The influence of the solvent on the electronic spectra of compound (2, MOFCA) for the calculated and experimental results is shown in Fig. 8a and b, respectively. Fig. 9 (a-c) show the charge density maps of the occupied and vacant MO's. The spectrum contains seven bands of non-polar solvents (dioxane, and toluene), which were observed at 500 nm and 450 nm and 435 nm and 375, 325, 280, and 255, respectively. The range of spectrum bands for the excited and the ground states have the same values when incident increasing the polarity of the solvent to (butanol and

methanol), also; the Intensity of the bands increases with polar solvents, so all the band's shifts to ($\pi-\pi^*$) and (n- π^*). A concourse between theoretical and experimental results is creating from the electron excitation of the ten MO molecular orbital's $\varphi_{59}^{-1}\varphi_{70} - \varphi_{71}^{-1}\varphi_{90}$, for MOFCA. Table S1 and Fig. 9 (a-c) give the first (n- π^*)¹ band in non-polar solvents (dioxane, and toluene), observed at (450, 450 nm), and theoretically at (500, 500 nm), through a configuration of $\varphi_{68-70}^{-1}\varphi_{71-74}$, 77, 80-86, 91, 99. Other sides, in polar solvents (butanol and methanol), at (411, 411 nm), band, where the computed bands at 460 and 460 nm, respectively. The electronic transformation indicated the features of the electron density are from the nature of the molecular orbital. Fig. 9 (a-c) apparent the delocalization of the electron density and the charge transfer characteristic. The absorption bands in the visible region are typical transitions of n- π^* and $\pi - \pi^*$.

3.9. The optical band gap of the presented structures

The main experimental optical parameter of the presented structures is the energy gap, E_g which can be obtained for the direct type transition by using the Eq. 6 [64]:

$$(\alpha E)^2 = A(E - E_g) \quad (6)$$

Where E is the incident photon energy and A is a constant. As observed from the Fig. S2, that the best fit of the most feasible transition supports the direct band transition. The values of E_g for every structure that resulting from $[(\alpha E)^2 \text{ vs } (E)]$ plots can be extracted from the extrapolation of linear parts of the curve for each case to $(\alpha h\nu)^2 = 0$ as shown in the Fig. S2. The obtained E_g value of compound (2, MOFCA) is 2.92 eV.

3.10. Thermodynamic properties

The Zero-Point Vibrational Energies (ZPVE), and the entropy, S_{Vib} (T), are thermal parameters which calculated by using B3LYP/6-311++G (d,p). To calculate the accurate value

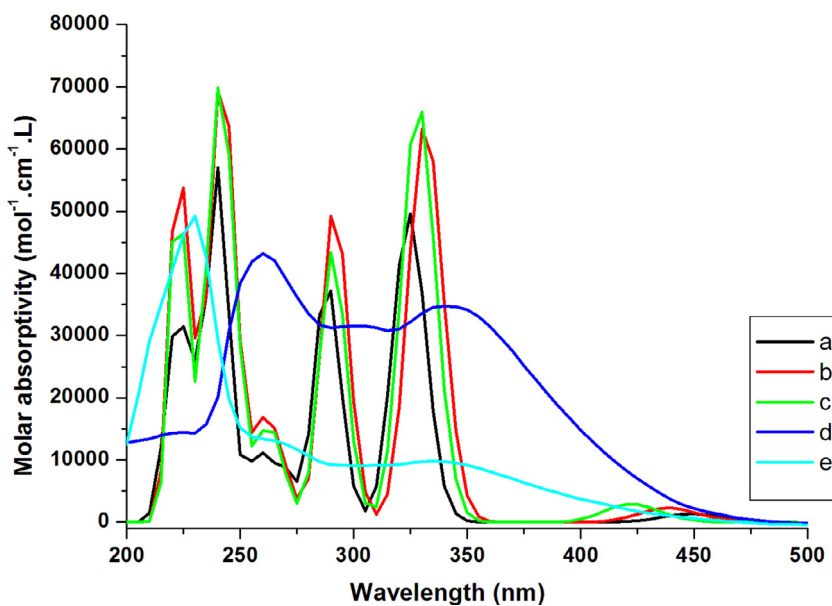
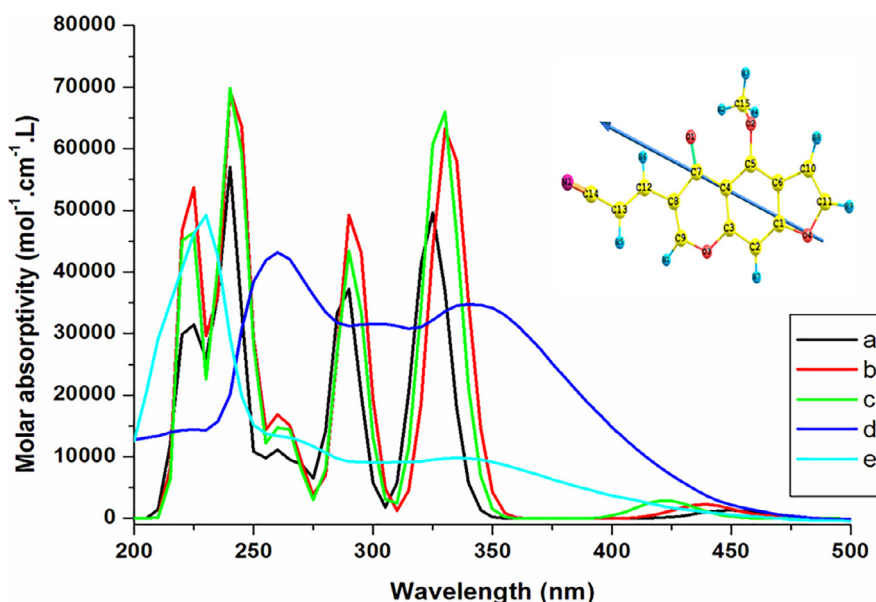


Fig. 8a. Electronic absorption spectra of compound (2, MOFCA), (a) theoretical in gas phase, (b) theoretical in dioxane, (c) theoretical in methanol (d) experimental in dioxane, (e) experimental in methanol.

of ZPVE of compound (**2, MOFCA**) by adding the scale factors value which equal 0.9804 at B3LYP/6-311++G (d,p) basis set. So; the accurate value of ZPVE of compound (**2, MOFCA**) is $129.875 \times 0.9804 = 127.330$ kcal.mol⁻¹, and total entropy is $132.509 \times 0.9804 = 129.912$ cal/mol. k, are also listed in Table 1.

Vibrational analysis and standard statistical thermodynamics functions, rule of, heat capacity (C_p^0, m), entropy (S_m^0), and enthalpy(H_m^0), for compound (**2, MOFCA**), were acquired at the B3LYP/6-311++G (d, p)level and are presented in Table 7. The intensities of the molecular vibration increase with the increasing temperature from 200.00 to 600.00 K, which ensues increasing in the standard heat capacities, entropies, and enthalpies. The correlations between these thermodynamic properties and temperatures T are given in Fig. S3. The correlation equations are as follows:

$$C_{p,m}^0 = 25.51733 + 0.14446T - 2.74133 \times 10^{-4}T^2; (R^2 = 0.99294), \quad (7)$$

$$S_m^0 = 78.3281 + 0.2206T + 1.74849 \times 10^{-5}T^2; (R^2 = 0.99876), \quad (8)$$

$$H_m^0 = 97.48244 - 0.08433T + 1.30194 \times 10^{-4}T^2; (R^2 = 0.99531). \quad (9)$$

These equations will be helpful for further studies for compound (**2, MOFCA**), [65,66].

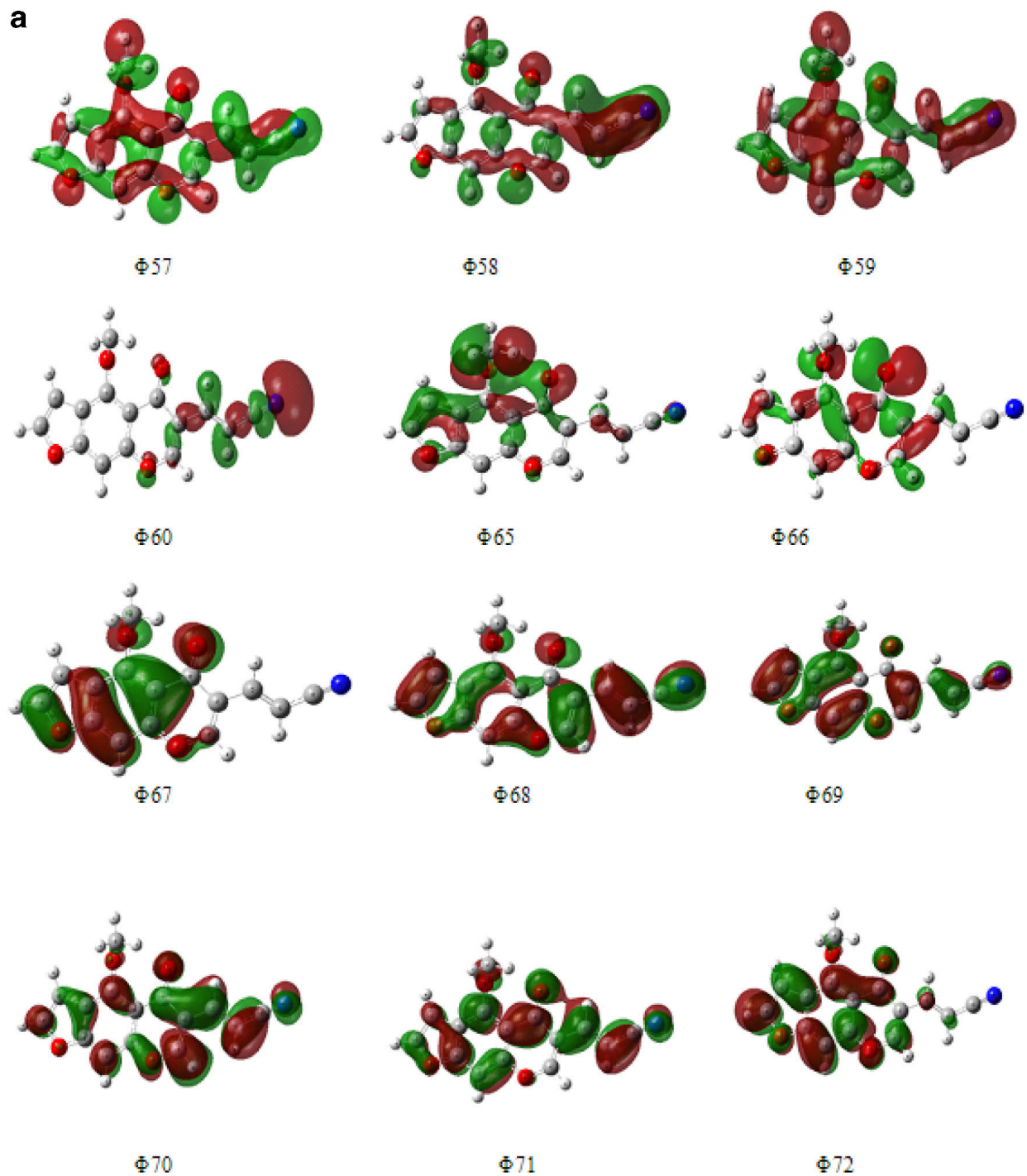


Fig. 8b. Electronic absorption spectra of compound (2, MOFCA), (a) theoretical in gas phase, (b) theoretical in toluene, (c) theoretical in butanol (d) experimental in toluene, (e) experimental in butanol.

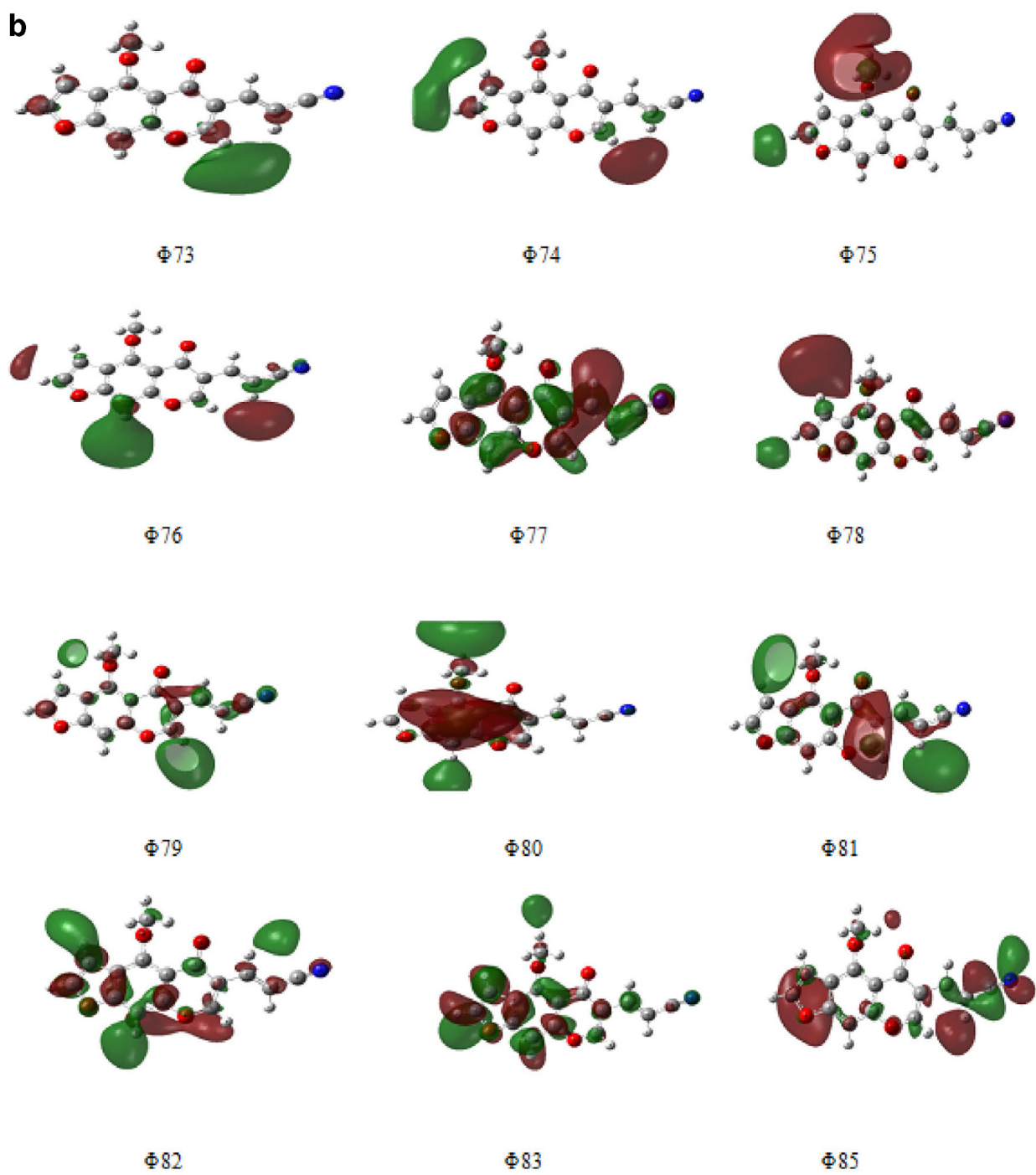


Fig. 8b. Continued

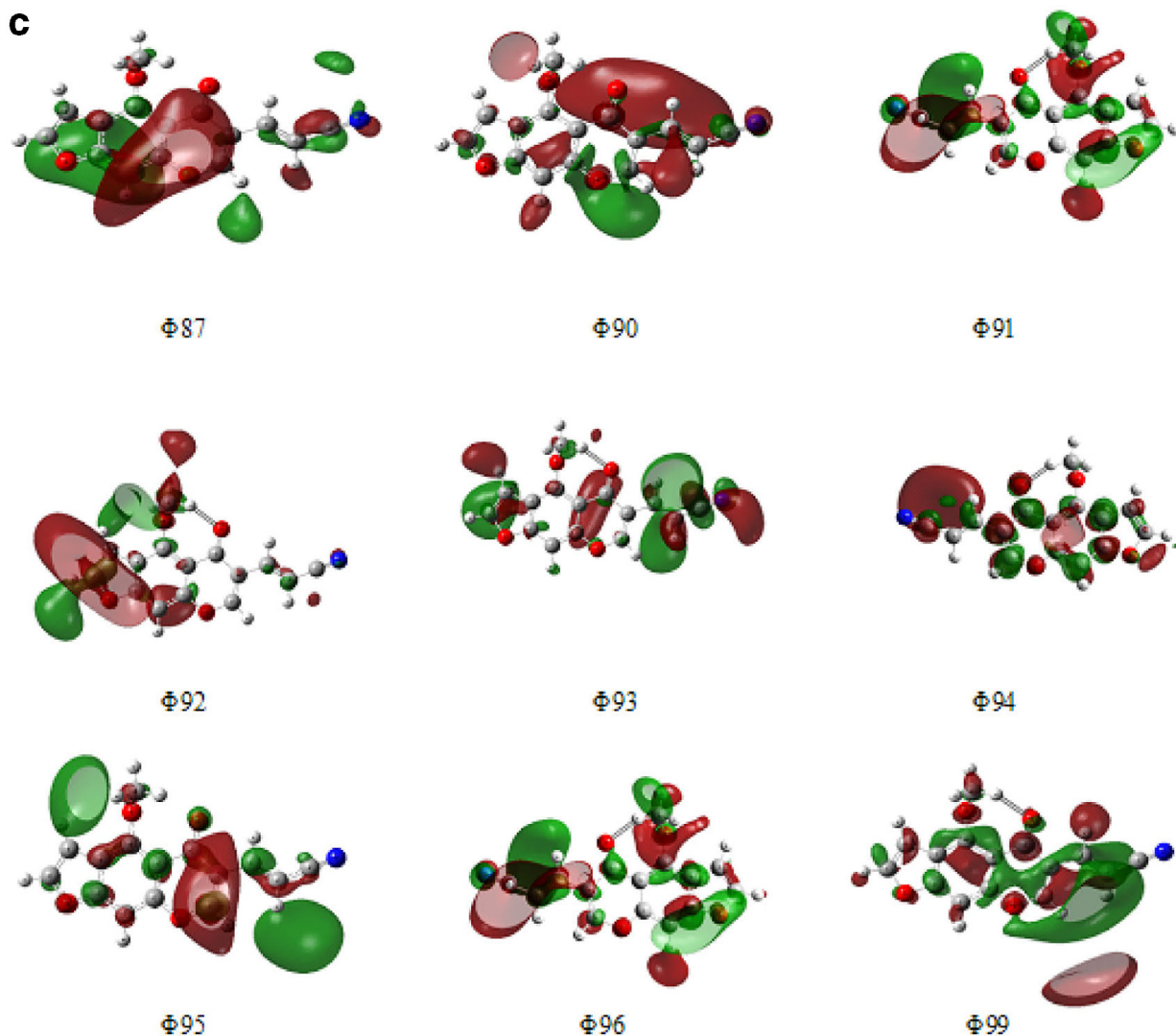


Fig. 9. (a-c). Electron density contours of compound (2, MOFCA).

4. Conclusion

A novel (*2E*)-3-(4-methoxy-5-oxo-5H-furo[3,2-g]chromen-6-yl)acrylonitrile (**2, MOFCA**) was obtained from reaction of 6-formylvisnagin and cyano acetic acid. The electronic geometrical structure of the studied compound (**2, MOFCA**) were investigated theoretically by using the DFT method at B3LYP/6-311++G (d, p), and TD-DFT at CAM/B3LYP/6-311++G (d, p) level theory. The UV-Vis analysis in **MOFCA** gave red and blue shifts of the absorption bands and revealed the occurrence of maximum excitations for ($n-\pi^*$ and $\pi-\pi^*$) transitions. While the experimental FT-IR spectra well copied by the DFT calculations. Synthesized molecule **MOFCA** is a chemically hard compound with greater kinetic stability and electron-donating capability as confirmed from global reactivity descriptors calculation and energy of FMO. The synthesized molecule has excellent uses in the technology-related applications, from NLO analysis which compared with urea molecule. The ESP and MEP maps show the charge distributions defining how molecules interact with each other and useful for visualizing the variable. As well; the electronic density has been connected to the dipole moments, electrical negativity, and the chemical reactivity of molecules. Furthermore, the thermodynamic parameters of the compound increase with the increasing temperature from 200.00 to 600.00 K.

Author agreement

Has not been previously published. Upon acceptance. The Author's name will always be included with the publication of the manuscript. The Author has the following nonexclusive rights: (1) to use the manuscript in the Author's teaching activities; (2) to publish the manuscript, or permit its publication, as part of any book the Author may write; and (3) to include the manuscript in the Author's own personal or departmental (but not institutional) database or on-line site; The Author also agrees to properly credit the journal as the original place of publication. These exclusive rights run the full term of the copyright and all renewals and extensions thereof. I hereby accept the terms of the above Author Agreement.

Declaration of Competing Interest

The authors declare that they have no known competing financial interests or personal relationships that could have appeared to influence the work reported in this paper.

Supplementary materials

Supplementary material associated with this article can be found, in the online version, at [doi:10.1016/j.molstruc.2020.129316](https://doi.org/10.1016/j.molstruc.2020.129316).

References

- [1] A.A. Abu-Hashem, M. El-Shazly, Synthesis, reactions and biological activities of furochromones: a review, *Eur. J. Med. Chem.* 90 (2015) 633–665.
- [2] H.A. Dewar, T.A. Grimson, Khellin in the treatment of angina of effort, *Br. Heart J.* 12 (1950) 54–60.
- [3] D. Vedaldi, S. Caffieri, F. Dall'Acqua, L. Andrea, L. Bovalini, P. Martelli, Khellin, a naturally occurring furochromone, used for the photo chemotherapy of skin diseases: mechanism of action, *Farmaco* 4 (1988) 333–346.
- [4] P. Vanachayangkul, K. Byer, S. Khan, V. Butterweck, An aqueous extract of Ammi visnaga fruits and its constituents khellin and visnagin prevent cell damage caused by oxalate in renal epithelial cells, *Phytomedicine* 17 (2010) 653–658.
- [5] M. Ghate, M.V. Kulkarni, Synthesis and anti-inflammatory activity of 4-(5-acetyl-6'-hydroxy-3'-methyl-benzofuran-2'-yl)coumarin and 6-acetyl-3,7-dimethyl-2-(coumarin-4'-yl)furo[3,2-g]chromen-5-one, *Indian J. Chem. A* 44B (2005) 1674–1678.
- [6] M.S. Frasinyuk, S.V. Gorelov, S.P. Bondarenko, V.P. Khilya, Synthesis and properties of 4-(3-amino-2-benzofuranyl)coumarins, *Chem. Heterocycl. Compds.* 45 (2009) 1261–1269.
- [7] I.F. Zaeid, A.M. Nasef, N.M. Fawzy, A.M. Soliman, M.M. E-Baroudy, A novel multi-component reaction of indoles and formyl furochromone was described for the synthesis of indoles derivatives with expected antitumor activity, *Int. J. Pharm. Sci. Rev. Res.* 30 (2015) 306–314.
- [8] K.M. Amin, Y.M. Syam, M. Anwar, H.I. Ali, T.M. Abdel-Ghani, A.M. Serry, Synthesis and molecular docking study of new benzofuran and furo[3,2-g]chromone-based cytotoxic agents against breast cancer and p38 α MAP kinase inhibitors, *Bioorg. Chem.* 76 (2018) 487–500.
- [9] F.A. Ragab, N.A. El-Sayed, A.A.M. Eissa, A.M. El Kerdawy, Synthesis and anticonvulsant activity of certain substituted furochromone, benzofuran and flavone derivatives, *Chem. Pharm. Bull.* 58 (2010) 1148–1156.
- [10] S. V.Laxmi, Y.T. Reddy, B.S. Kuarm, P.N. Reddy, P.A. Crooks, B. Rajitha, Synthesis and evaluation of chromenyl barbiturates and thiobarbiturates as potential antitubercular agents, *Bioorg. Med. Chem. Lett.* 21 (2011) 4329–4331.
- [11] S.J. Beula, D.R. Suthakaran, M.B. Prakash, G. Sreeya, P.P. Kalyan, P.S. Prasad, Synthesis, characterization and antimicrobial activity of 7'-methyl 3-phenyl-2,3-dihydro-4'-furochromene, *Asian J. Pharm. Tech.* 10 (2020) 85–89.
- [12] I.O. Akchurin, A.I. Yakhutina, A.Y. Bochkov, N.P. Solovjova, M.G. Medvedev, V.F. Traven, Novel push-pull fluorescent dyes 7-(diethylamino)-furo-and thieno[3,2-c]coumarins derivatives: structure, electronic spectra and TD-DFT study, *J. Mol. Struct.* 1160 (2018) 215–221.
- [13] M.A. Ibrahim, S. Abdel Halim, N. Roushdy, A.A.M. Farag, N.M. El-Gohary, Synthesis, DFT band structure calculations, optical and photoelectrical characterizations of the novel 5-hydroxy-4-methoxy-7-oxo-7H-furo[3,2-g]chromene 6-carbonitrile (HMOFCC), *Opt. Mater.* 73 (2017) 290–305.
- [14] N. Roushdy, A.A.M. Farag, M.A. Ibrahim, S. Abdel Halim, N.M. El-Gohary, Synthesis, spectral characterization, DFT and photosensitivity studies of 1-[(4 methoxy-5-oxo-5H-furo[3,2-g]chromen-6-yl)methylidene]amino-4,6-dimethyl-2-oxo-1,2-dihydropyridine-3-carbonitrile (MFCMP), *Optik* 178 (2019) 1163–1176.
- [15] A.A.M. Farag, M.A. Ibrahim, S. Abdel Halim, N. Roushdy, N.M. El-Gohary, Synthesis, DFT calculations, spectroscopic and photovoltaic of the novel N", N"- bis([(4,9-dimethoxy-5-oxo-5H-furo[3,2-g]chromen-6-yl)methylidene]thiocarbono-hydrazide (BFCMT) and its photodiode application, *J. Mol. Struct.* 1156 (2018) 516–523.
- [16] M.A. Ibrahim, S. Abdel Halim, N. Roushdy, A.A.M. Farag, N.M. El-Gohary, Synthesis, DFT study and photoelectrical characterizations of the novel 4-methoxyfuro[3',2':6,7]chromeno[2,3-e]benzo[b][1,4]diazepin-5(1H)-one, *Optik* 166 (2018) 294–306.
- [17] C.V. Maridevarmath, L. Naik, V.S. Negalurmath, M. Basanagouda, G.H. Malimath, Synthesis, photophysical, DFT and solvent effect studies on biologically active benzofuran derivative: (5-methyl-benzofuran-3-yl)-acetic acid hydrazide, *Chem. Data Collect.* 21 (2019) 100221.
- [18] C.V. Maridevarmath, L. Naik, V.S. Negalurmath, M. Basanagouda, G.H. Malimath, Synthesis, characterization and photophysical studies on novel benzofuran-3-acetic acid hydrazide derivatives by solvatochromic and computational methods, *J. Mol. Struct.* 1188 (2019) 142–152.
- [19] D. Coskun, B. Gunduz, M.F. Coskun, Synthesis, characterization and significant optoelectronic parameters of 1-(7-methoxy-1-benzofuran-2-yl) substituted chalcone derivatives, *J. Mol. Struct.* 1178 (2019) 261–267.
- [20] M.A. Ibrahim, N.M. El-Gohary, Domino reactions between 3-(6-methyl chromonyl)acrylonitrile and nucleophilic reagents, *Tetrahedron* 74 (2018) 512–518.
- [21] D. Tuncel, π -Conjugated nanostructures materials: preparation, properties, and Photonic applications, *Nanoscale Adv.*, 1 (2019) 19–33.
- [22] S. Abdel Halim, M.A. Ibrahim, Synthesis, DFT calculations, electronic structure, electronic absorption spectra, natural bond orbital (NBO) and nonlinear optical (NLO) analysis of the novel 5-methyl-8H-benzo[h]chromeno[2,3-b][1,6] naphthyridine-6(5H),8-dione (MBCND), *J. Mol. Struct.* 1130 (2017) 543–558.
- [23] S. Abdel Halim, M.A. Ibrahim, Synthesis, density functional theory band structure calculations, optical, and photoelectrical characterizations of the novel (9-bromo-3-cyano-5-oxo-1,5-dihydro-2h-chromeno[4,3-b]pyridin-2-ylidene)propanedinitrile, *J. Heterocycl. Chem.* 56 (2019) 2542–2554.
- [24] Y. Suzuki, T. Suzuki, Gold nanoparticles in chemical and biological sensing, *J. Phys. Chem. A* 112 (2008) 402–411.
- [25] A.W. Potts, D.M.P. Holland, A.B. Trofimov, J. Schirmer, L. Karlsson, K. Siegbahn, Development and application of the quantum chemical method of Green's functions, *J. Phys. B* 36 (2003) 3129–3141.
- [26] M.E. KSahin, M. Cinar, I. Erol, M. Kurt, X-ray, FT-Raman, FT-IR spectra and ab initio HF, DFT calculations of 2-[(5-methylisoxazol-3-yl)amino]-2-oxo-ethyl methacrylate, *J. Mol. Struct.* 886 (2008) 148–157.
- [27] S. Abdel Halim, I.A. Laila, S.G. Sanad, Theoretical calculations of solvation 12-crown-4 (12CN4) in aqueous solution and its experimental interaction with nano CuSO₄, *Int. J. Nano Dimens.* 8 (2017) 142–158.
- [28] D.M.P. Holland, L. Karlsson, W. von Niessen, the identification of the outer valence shell π -photoelectron bands in furan, pyrrole and thiophene, *J. Electron. Spectrosc. Relat. Phenom.* 113 (2001) 221–239.
- [29] S. Abdel Halim, A.K. Khalil, TD-DFT calculations, NBO analysis and electronic absorption spectra of some thiazolo[3,2-a]pyridine derivatives, *J. Mol. Struct.* 1147 (2017) 651–667.
- [30] M. Karabacak, M. Cinar, Z. Unal, M. Kurt, FT-IR, UV spectroscopic and DFT quantum chemical study on the molecular conformation, vibrational and electronic transitions of 2-aminoterephthalic acid, *J. Mol. Struct.* 982 (2010) 22–27.
- [31] M. Kurt, T.R. Sertbakan, M. Ozdurhan, M. Karabacak, Infrared and Raman spectrum, molecular structure and theoretical calculation of 3, 4 dichlorophenylboronic acid, *J. Mol. Struct.* 921 (2009) 178–187.
- [32] M. Govindarajan, K. Ganasan, S. Periandy, M. Karabacak, Experimental (FT-IR and FT-Raman), electronic structure and DFT studies on 1-methoxynaphthalene, *Spectrochim. Acta. A* 79 (2011) 646–653.
- [33] M. Govindarajan, M. Karabacak, FT-IR, FT-Raman and UV spectral investigation; computed frequency estimation analysis and electronic structure calculations on 4-hydroxypyridine, *J. Mol. Struct.* 1038 (2013) 114–125.
- [34] M. Karabacak, M. Cinar, M. Kurt, DFT based computational study on the molecular conformation, NMR chemical shifts and vibrational transitions for N-(2 methylphenyl) methanesulfonamide and N-(3-methylphenyl) methanesulfonamide, *J. Mol. Struct.* 968 (2010) 108–114.
- [35] M. Frisch, J.G.W. Trucks, H.B. Schlegel, G.E. Scuseria, et al., Gaussian, Inc., Wallingford CT, (2009).
- [36] (a) A.D. Becke, A new mixing of Hartree–Fock and local density-functional theories, *J. Chem. Phys.* 98 (1993) 1372–1376; (b) A. D.Becke, Density functional thermochemistry, III: the role of exact exchange, *J. Chem. Phys.* 98 (1993) 5648–5652.
- [37] (a) C. Lee, W. Yang, R. G.Parr, Development of the Colle-Salvetti correlation-energy formula into a functional of the electron density, *Phys. Rev. B Condens. Matter* 37 (1988) 785–789; (b) B. Miehlich, A. Savin, H. Stolt, H. Preuss, Results obtained with the correlation energy density functional of Becke and Lee, Yang and Parr, *Chem Phys. Lett.* 157 (1989) 200–206.
- [38] B. Stefanov, G. Liu, A. Liashenko, P. Piskorz, I. Komaromi, R.L. Martin, D.J. Fox, T. Keith, A.M. Al-Laham, C.Y. Peng, A. Nanayakkara, M. Challacombe, P.M.W. Gill, B. Johnson, W. Chen, M.W. Wong, C. Gonzalez, J.A. Popple, Gaussian, Inc., Pittsburgh PA, (2003).
- [39] R. Dennington, T.M. Keith, *Gauss View, Version 5*, J. Semichem Inc., Shawnee Mission KS, 2009.
- [40] <http://www.chemcraftprog.com>.
- [41] D. Avci, Second and third-order nonlinear optical properties and molecular parameters of azo chromophores: semiempirical analysis, *SpectrU* 82 (2011) 37–43.
- [42] D. Avci, A. Baþoglu, Y. Atalay, Ab initio HF and DFT calculations on an organic non-linear optical material, *Struct. Chem.* 21 (2010) 213–219.
- [43] D. Avci, H. Cömert, Y. Atalay, Ab initio Hartree-Fock calculations on linear and second-order nonlinear optical properties of new acridine-benzothiazolylamine chromophores, *J. Mol. Mod.* 14 (2008) 161–169.
- [44] V.R.T. Verbiest, K. Clays, CRC Press, New York, (2009).
- [45] A. Politano, G. Chiarello, V. Formoso, R.G. Agostino, E. Colavita, Plasmon of Shockley surface states in Cu(111): a high-resolution electron energy loss spectroscopy study, *J. Phys. Rev. B* 74 (R) (2006) 8–15 081401.
- [46] R.G. Pearson, Absolute electronegativity and hardness correlated with molecular orbital theory, *Proc. Nat. Acad. Sci.* 83 (1986) 8440–8441.
- [47] A.K. Chandra, T. Uchimura, Hardness profile: a critical study, *J. Phys. Chem. A* 105 (2001) 3578–3582.
- [48] J.G. Matecki, Phosphoinositides: tiny lipids with giant impact on cell regulation, *Trans. Met. Chem.* 35 (2010) 801–811.
- [49] T. Yanai, D. Tew, N.A. Handy, New hybrid exchange–correlation functional was using the Coulomb-attenuating method (CAM-B3LYP), *Chem. Phys. Lett.* 393 (2004) 51–57.
- [50] J.N. Macdonald, S.A. Mackay, J.K. Tyler, A.P. Cox, I.C. Ewart, Orientation in the addition of HD molecules to buta-1,3-diene over ZnO catalyst. A method of judging heterolytic and homolytic dissociation of hydrogen in catalysis, *J. Chem. Soc. Faraday Trans. II* 77 (1981) 79–89.
- [51] D. Sajan, Y. Erdogdu, R. Reshma, O. Dereli, K. Thomas, K.I. Hubert, Systematic ab initio gradient calculation of molecular geometries, force constants, and dipole moment derivatives, *Spectrochimica. Acta. Part. A* 82 (2011) 118–128.
- [52] N.M. Young, J.R. Brisson, J. Kelly, D.C. Watson, L. Tessier, P.H. Lanthier, H.C. Jarrell, N. Cadotte, F.S. Michael, E. Aberg, C.M. Szymanski, Structure of the N-linked glycan present on multiple glycoproteins in the Gram-negative bacterium, *Campylobacter jejuni*, *J. Biol. Chem.* 277 (2002) 42530–42539.
- [53] T. Asano, A. Sakai, S. Ouchi, M. Sakaida, A. Miyazaki, S. Hasegawa, Solid halide electrolytes with high lithium-ion conductivity for application in 4 V class bulk-type all-solid-state batteries, *Adv. Mater.* 30 (2018) 1803075–1803082.

- [54] S. Fatma, A. Bishnoi, A.K. Verma, Synthesis, spectral analysis (FT-IR, ^1H NMR, ^{13}C NMR and UV-visible) and quantum chemical studies on molecular geometry, NBO, NLO, chemical reactivity and thermodynamic properties of novel 2-amino-4-(dimethylamino)phenyl)-5-oxo-6-phenyl-5,6-dihydro-4H-pyran[3,2]cquinoline-3-carbonitrile, *J. Mol. Struct.* 1095 (2015) 112–124.
- [55] W.M.I. Hassan, H. Moustafa, M.N.H. Hamed, L.I. Ali, S. Abdel Halim, DFT calculations and electronic absorption spectra of some, α - and γ -pyrone derivatives, *Spectrochimica Acta*, 117 (2014) 587–597.
- [56] M. Khalid, M.A. Ullah, M. Adeel, M.U. Khan, M.N. Tahir, A. Albert, C. Braga, Synthesis, crystal structure analysis, spectral IR, UV-Vis, NMR assessments, electronic and nonlinear optical properties of potent quinoline based derivatives: interplay of experimental and DFT study, *J. Saudi Chem. Soc.* 23 (2019) 546–560.
- [57] J.S. Murray, K. Sen, Molecular electrostatic potentials, concepts and applications, Elsevier, Amsterdam 7 and E. Scrocco, J. Tomasi, electronic molecular structure, reactivity and intermolecular forces: an heuristic interpretation by means of electrostatic molecular potentials, *Adv. Quant. Chem.* 11 (1996) 115–193.
- [58] P. Politzer, J.S. Murray, the fundamental nature and role of the electrostatic potential in atoms and molecules, *Theor. Chem. Acc.* 108 (2002) 134–142.
- [59] D. Sajan, L. Joseph, N. Vijayan, M. Karabacak, Natural bond orbital analysis, electronic structure, non-linear properties and vibrational spectral analysis of L-histidinium bromide monohydrate: a density functional theory, *Spectrochim. Acta A* 81 (2011) 85–98.
- [60] J. Chocholoušová, V. Špirko, P. Hobza, First local minimum of the formic acid dimer exhibits simultaneously red-shifted O–H...O and improper blue-shifted C–H...O hydrogen bonds, *Phys. Chem. A* 6 (2004) 37–41.
- [61] M. Szafran, A. Komasa, E. Bartoszak-Adamska, Crystal and molecular structure of 4-carboxypiperidinium chloride (4-piperidinecarboxylic acid hydrochloride), *J. Mol. Struct.* 827 (2007) 101–107.
- [62] J.B. Lambert, H.F. Shurvell, L. Vereit, R.G. Cooks, G.H. Stout, *Organic Structural Analysis*, Academic Press, New York, 1976.
- [63] P.S. Kalsi, *Spectroscopy of Organic Compounds*, Academic Press, New York, 2002.
- [64] K. Hemalatha, S.K. Rukmani, N. Suriyamurthy, B.M. Nagabhushana, Scheelite-type MWO_4 ($M = \text{Ca}, \text{Sr}, \text{and Ba}$) nanophosphors: facile synthesis, structural characterization, photoluminescence, and photocatalytic properties, *Mater. Res. Bull.* 51 (2014) 438–448.
- [65] H. Tanak, Molecular structure, spectroscopic (FT-IR and UV-Vis) and DFT quantum-chemical studies on 2-[2,4-Dimethylphenyl]iminomethyl]-6-methylphenol, *Mol. Phys.* 112 (2014) 1553–1565.
- [66] H. Tanak, M.K. Marchewka, M. Drozd, Molecular structure and vibrational spectra of Bis(melaminium)terephthalate dihydrate: a DFT computational study, *Spectrochim. Acta A* 105 (2013) 156–164.